

New Porphyrin-Based Metal–Organic Framework with High Porosity: 2-D Infinite 22.2-Å Square-Grid Coordination Network

Tetsushi Ohmura,^{*,†} Arimitsu Usuki,[†] Kenzo Fukumori,[†] Takashi Ohta,[†] Mikinao Ito,[‡] and Kazuyuki Tatsumi[‡]

Toyota Central R&D Laboratories, Inc., 41-1 Yokomichi, Nagakute, Nagakute-cho, Aichi-gun, Aichi 480-1192, Japan, and Research Center for Materials Science and Department of Chemistry, Graduate School of Science, Nagoya University, Furo-cho, Chikusa-ku, Nagoya, Aichi 464-8602, Japan

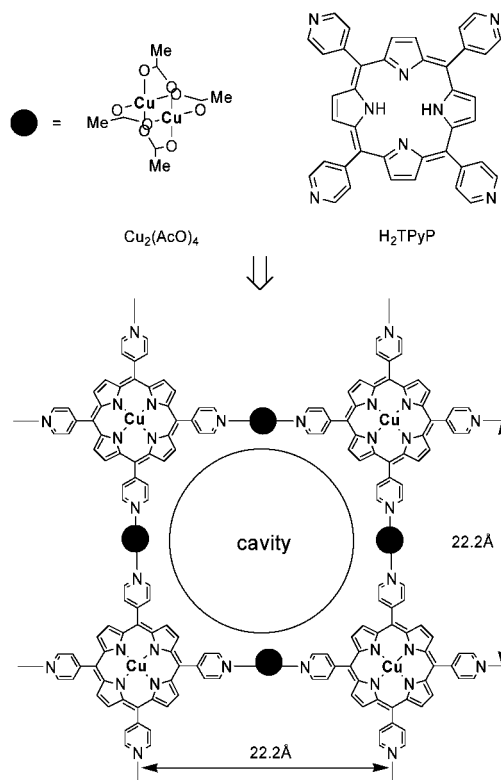
Received March 3, 2006

A new 2-D coordination network with 22.2-Å square-grid coordination networks was prepared from a dicopper(II) tetraacetate [Cu₂(AcO)₄] as a linear linker motif and 5,10,15,20-tetra-4-pyridyl-21*H*,23*H*-porphine (H₂TPyP) as a four-connected vertex, forming a regular high-porous structure. The characterization by N₂ adsorption indicated that this coordination network has uniform micropores and gas adsorption cavities.

Metal–organic frameworks (MOFs) with cavities have been subjected to intensive study for the past decade.¹ Such materials have been extensively studied in recent years because of their intriguing structures and, more importantly, for their potential applications in gas storage, molecular sieves, ion exchange, and catalysis.² This class of porous coordination networks is obtained through the selection of metal and ligand sets based on their coordination tendencies and geometries.

Previous studies have demonstrated that dinuclear metal carboxylates construct 1-D channels to utilize the H bond and/or π – π -stacking capabilities of suitable organic ligands.³ Additionally, previous studies have demonstrated the formation of infinite porphyrin-based MOFs using 5,10,15,20-tetra-

Scheme 1. Construction of a Porous Coordination Network



4-pyridyl-21*H*,23*H*-porphine (H₂TPyP) and mononuclear metal (Hg,^{4a} Co,^{4b} Fe,^{4c} Mn,^{4d} and Zn^{4d,e}) as a linker.

* To whom correspondence should be addressed. E-mail: e1314@mosk.tytlabs.co.jp.

[†] Toyota Central R&D Laboratories, Inc.

[‡] Nagoya University.

- (1) (a) Mori, W.; Inoue, F.; Yoshida, K.; Nakayama, H.; Takamizawa, S.; Kishita, M. *Chem. Lett.* **1997**, 1219–1220. (b) Li, H.; Eddaoudi, M.; Groy, T. L.; Yaghi, O. M. *J. Am. Chem. Soc.* **1998**, *120*, 8571–8572. (c) Kitagawa, S.; Kondo, M. *Bull. Chem. Soc. Jpn.* **1998**, *71*, 1739–1753.
- (2) (a) Rowsell, J. L. C.; Eckert, J.; Yaghi, O. M. *J. Am. Chem. Soc.* **2005**, *127*, 14904–14910. (b) Perles, J.; Iglesias, M.; Luengo, M.-A. M.; Monge, M. A.; Valero, C. R.; Snejko, N. *Chem. Mater.* **2005**, *17*, 5837–5842. (c) Sun, D.; Ke, Y.; Mattox, T. M.; Ooro, B. A.; Zhou, H.-C. *Chem. Commun.* **2005**, 5447–5449. (d) Sudik, A. C.; Millward, A. R.; Ockwig, N. W.; Côté, A. P.; Kim, J.; Yaghi, O. M. *J. Am. Chem. Soc.* **2005**, *127*, 7110–7118. (e) Férey, G.; Draznieks, C. M.; Serre, C.; Millange, F.; Dutour, J.; Surblé, S.; Margiolaki, I. *Science* **2005**, *309*, 2040–2042. (f) Seo, J. S.; Whang, D.; Lee, H.; Jun, S. I.; Oh, J.; Jeon, Y. J.; Kim, K. *Nature* **2000**, *404*, 982–986.

- (3) (a) Nukada, R.; Mori, W.; Takamizawa, S.; Mikuriya, M.; Handa, M.; Naono, H. *Chem. Lett.* **1999**, 367–368. (b) Wang, X.; Guo, Y.; Li, Y.; Wang, E.; Hu, C.; Hu, N. *Inorg. Chem.* **2003**, *42*, 4135–4140. (c) Takamizawa, S.; Nakata, E.; Yokoyama, H. *Inorg. Chem. Commun.* **2003**, *6*, 763–765.
- (4) (a) Carlucci, L.; Ciani, G.; Proserpio, D. M.; Porta, F. *Angew. Chem., Int. Ed.* **2003**, *42*, 317–322. (b) Pan, L.; Huang, X.; Phan, H.-L. N.; Emge, T. J.; Li, J.; Wang, X. *Inorg. Chem.* **2004**, *43*, 6878–6880. (c) Hagrman, D.; Hagrman, P. J.; Zubieta, J. *Angew. Chem., Int. Ed.* **1999**, *38*, 3165–3168. (d) Krishna Kumar, R.; Goldberg, I. *Angew. Chem., Int. Ed.* **1998**, *37*, 3027–3030. (e) Deiters, E.; Bulach, V.; Hosseini, M. W. *Chem. Commun.* **2005**, 3906–3908.

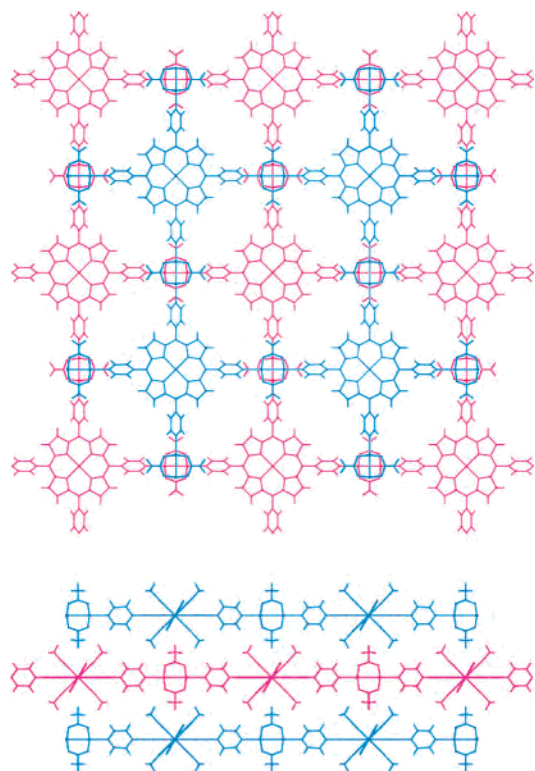


Figure 1. Crystal packing diagram of **1** showing three sets of 2-D arrays colored alternately. Guest solvents are omitted for clarity.

In this Communication, we report the synthesis and characterization of a new porphyrin-based MOF consisting of CuTPyP and a dicopper cluster as a linker.

The reaction of H₂TPyP with dicopper(II) tetraacetate [Cu₂(AcO)₄] produces the first porphyrin-based MOF. Formulated empirically as [Cu₂(AcO)₄(CuTPyP)_{1/2}]·CHCl₃ (**1**), which exhibits a 2-D infinite 22.2-Å square-grid coordination

network consisting of CuTPyP linked by Cu₂(AcO)₄, the structural motif is displayed in Scheme 1. The structure of **1** was determined via single-crystal X-ray diffraction (XRD) analysis.⁵

The distances of the square grid of **1**, with a dinuclear metal as the linker, were longer than those with a mononuclear metal unit as the linker.⁴ All four pyridyl groups of CuTPyP are coordinated to independent dinuclear metals of Cu₂(AcO)₄, the result of which is an undistorted square-grid 2-D network. Figure 1 shows one of the regular 2-D sheets in **1**. The Cu–Cu distance of 2.5986(15) Å for **1** is slightly shorter than the corresponding distance in [Cu₂(BDA)₂(H₂O)₂](MeOH)₂(H₂O)₄ [2.66(1) Å]⁶ or [Cu₂(O₂CMe)₄(4,4'-tpcb)_{1/2}](C₆H₆)₃ [2.600(1) Å].⁷ The Cu–N_{axial} distance for **1** is 2.148(8) Å, which is typical of such interactions.⁷ The 2-D layers stack along the *c* axis, with an interlayer separation of $\frac{1}{2}c$ (ca. 7.12 Å) and in an ABAB sequence (Figure 1). The structural networks do not interpenetrate. The structure does not show wide channels when viewed in the stacking direction because the larger squares of adjacent layers are not aligned. However, channels that run along an orientation that is inclined with respect to the planes of the layers, that is, along the corresponding planes, can be observed. These channels show five types of cross sections for various pore distributions when the van der Waals radii are considered as follows: an elliptical section of ca. 4.4 × 9.5 Å along [001] (Figure 2a), an elliptical section of ca. 1.6 × 3.5 Å along [010] (Figure 2b), a cruciform section of ca. 5.3 × 8.3 Å along [011] (Figure 2c), a cruciform section of ca. 3.0 × 7.6 Å along [110] (Figure 2d), and a circular section of ca. 6.7 × 7.4 Å along [111] (Figure 2e).

A thermogravimetric analysis of **1** in a He flow was performed. The sample mass first decreases by ca. 22 wt %

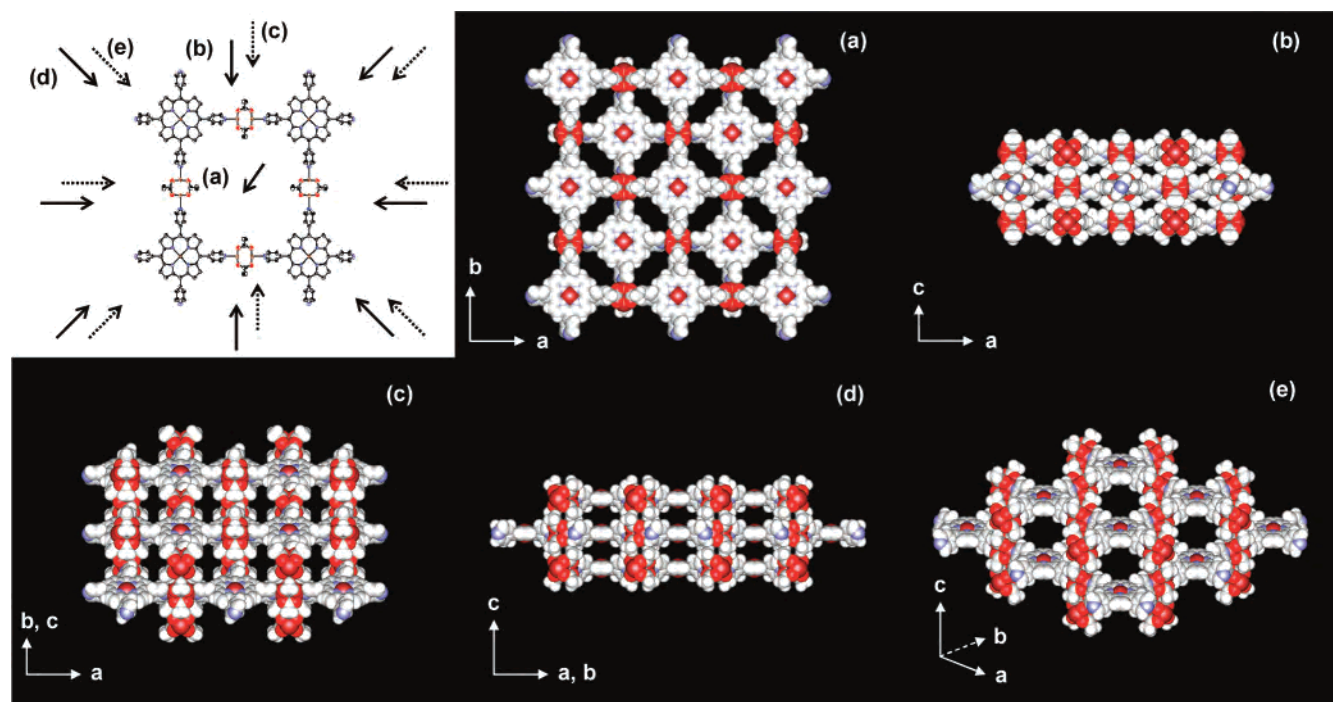


Figure 2. Space-filling view of **1** shown down the five directions (guest solvents are omitted for clarity), where open channels of (a) 4.4 × 9.5 Å, (b) 1.6 × 3.5 Å, (c) 5.3 × 8.3 Å, (d) 3.0 × 7.6 Å, and (e) 6.7 × 7.4 Å are partly occupied by a guest solvent.

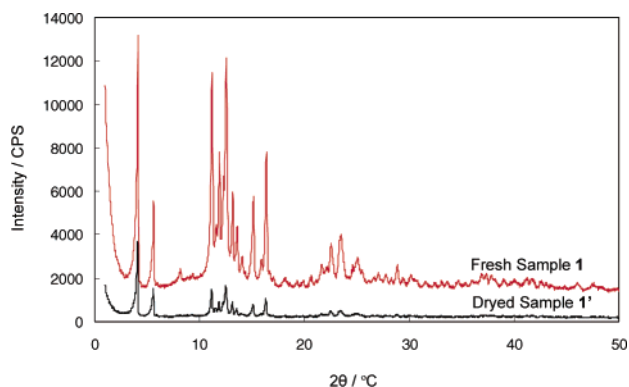


Figure 3. XRD patterns for **1** and **1'** showing that **1'** indicates the retention of crystallinity in the absence of guest molecules.

at 33–140 °C, and then a second decrease of ca. 22 wt %, with respect to the initial mass, occurs at 140–315 °C. The second weight loss gives rise to decomposition of the frameworks because $\text{Cu}_2(\text{AcO})_4$ is the linker between the CuTPyPs and plays an important role in retaining the cavity.⁸

Evacuation of **1** at room temperature generates $[\text{Cu}_2(\text{AcO})_4(\text{CuTPyP})_{1/2}]$ (**1'**), which retains a crystallinity, as shown by a powder XRD pattern, that is consistent with that of **1** (Figure 3) and exhibits high gas-occlusion properties.

The adsorption and desorption isotherms of **1'** are shown in Figure 4.⁹ The adsorption of N_2 follows a type I¹¹ isotherm with a Brunauer–Emmett–Teller surface area of 812.08 $\text{m}^2 \text{g}^{-1}$, a Langmuir surface area of 1035.96 $\text{m}^2 \text{g}^{-1}$, and a

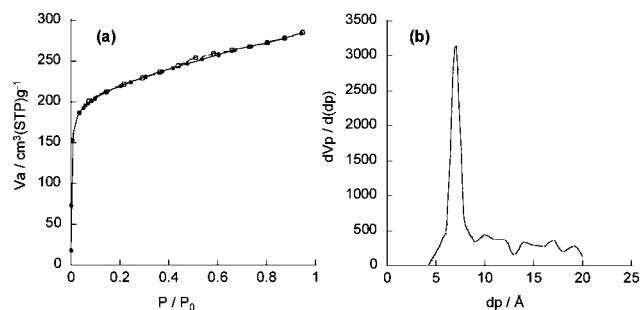


Figure 4. (a) N_2 adsorption (●) and desorption (○) isotherms for **1'** measured volumetrically at 77 K. (b) Micropore size distributions for **1'** calculated by the MP method from the adsorption isotherms.¹⁰

micropore volume of 0.4737 $\text{cm}^3 \text{g}^{-1}$, which are significantly higher than those of any porphyrin-based MOFs reported to date under the same conditions.¹²

In summary, we have synthesized the first porphyrin-based MOF supported by H_2TPyP and $\text{Cu}_2(\text{AcO})_4$. The porous structure of **1**, which is constructed by the self-assembly of a 2-D coordination network consisting of a 22.2-Å square grid, was determined by X-ray crystallography. The structural motif of **1** appears to explain the retention of crystallinity in **1'** and has a high surface area and micropore volume characterized by N_2 adsorption measurement. Further studies will include an investigation into H_2 storage, separation, catalysis, and molecular recognition, as well as an extension of supramolecular chemistry. The synthesis and characterization of porphyrin-based MOF styles with more extended dinuclear metals as the linker are in progress.

Acknowledgment. We gratefully thank Professor Dr. Wasuke Mori (Department of Chemistry, Faculty of Science, Kanagawa University), Dr. Tadao Ogawa (Toyota Central R&D Laboratories, Inc.) for helpful discussion, and Tomoyuki Kayama (Toyota Central R&D Laboratories, Inc.) for performing the thermogravimetry/gas chromatography–mass spectrometry (TG/GC–MS) measurements.

Supporting Information Available: Synthesis, IR, and TG/GC–MS details (PDF). This material is available free of charge via the Internet at <http://pubs.acs.org>.

IC060358H

(5) X-ray single-crystal diffraction data for **1** were collected on a Rigaku Mercury CCD diffractometer at -160 °C. Crystal data for **1**: tetragonal, space group $I4/mmm$, $a = b = 22.240(8)$ Å, $c = 14.232(6)$ Å, $V = 7040(5)$ Å³, $Z = 16$, $\rho_{\text{calcd}} = 0.792$ g cm^{-3} , $2\theta = 55^\circ$, Mo $K\alpha$ radiation ($\lambda = 0.71070$ Å); least-squares refinement based on 2286 reflections with final $R1 = 0.124$, $wR2 = 0.169$, and $\text{GOF} = 1.359$.

(6) Cui, Y.; Ngo, H. L.; White, P. S.; Lin, W. *Chem. Commun.* **2003**, 994–995.

(7) Papaefstathiou, G. S.; MacGillivray, L. R. *Angew. Chem., Int. Ed.* **2002**, *41*, 2070–2073.

(8) The TG/GC–MS analyses of **1** are given in Supporting Information Figure 1S. To provide a clear presentation of the MS profile curves, numerous different fragments have been selected and displayed.

(9) For **1'**, a N_2 adsorption experiment was carried out in the relative pressure range from 10^{-6} to 1 using a BelJapan Belsorp 18 Plus adsorption apparatus.

(10) Mikhail, R. Sh.; Brunauer, S.; Bodor, E. E. *J. Colloid Interface Sci.* **1968**, *26*, 45–53.

(11) Sing, K. S.; Everett, D. H.; Haul, R. A. W.; Moscou, L.; Pierotti, R. A.; Rouquerol, J.; Siemieniewska, T. *Pure Appl. Chem.* **1985**, *57*, 603–619.

(12) (a) Sato, T.; Mori, W.; Kato, C. N.; Ohmura, T.; Sato, T.; Yokoyama, K.; Takamizawa, S.; Naito, S. *Chem. Lett.* **2003**, *32*, 854–855. (b) Sato, T.; Mori, W.; Kato, C. N.; Yanaoka, E.; Kuribayashi, T.; Ohtera, R.; Shiraishi, Y. *J. Catal.* **2005**, *232*, 186–198.